

EFFECT OF INCLUSIONS AND DISSOLVED HYDROGEN ON THE FRACTURE TOUGHNESS OF PIPELINE STEELS

J.M. Hallen¹ J.L. González¹ J. Hernández¹ and F Hernández-Lagos²

¹Instituto Politécnico Nacional, ESIQIE, Dep. de Ing Metalúrgica
Labs. de Metalurgia, Apdo. Post. 75-872, México, D.F. 07300 MEXICO

²Subgerencia de Mantenimiento a Ductos e Instalaciones, PEMEX Exploración Producción Región Sur
Edif. 4 Centro Técnico Administrativo, Av. Carrizal Esq. Campo Samaria, Villahermosa, Tabasco.

ABSTRACT

The purpose of this work was to investigate the role of the shape and amount of sulfide inclusions, and dissolved hydrogen on the fracture toughness of API X-52 pipeline steels. The shape and amount of inclusions was controlled by adding calcium and varying the sulfur content from 0.002 to 0.030 weight percent. Fracture toughness was evaluated using compact tensile specimens and hydrogen charging was carried out in NACE H₂S solution varying the charging time from 12 to 72 hours. The addition of hydrogen reduced the fracture toughness of the pipeline steels. The fracture surface of uncharged specimens was ductile, while the fracture surface of hydrogen charged specimens was a mixture of cleavage and ductile. Hydrogen embrittlement was related to the sulfur content and the shape of the inclusions. The results of this work suggest that controlling the shape of the sulfide inclusions to the spherical type by addition of calcium is not enough to minimize the detrimental effect of hydrogen on fracture toughness of pipeline steels, but at the same time the volume fraction of non metallic inclusions has to be controlled, even if they have a spherical shape.

I. INTRODUCTION

Prominent improvements have been made in manufacturing high performance line-pipes to cope with severe service conditions such as the transport of natural hydrocarbons containing hydrogen sulfide (sour hydrocarbons)^{1,2}. Strict requirements for mechanical properties, weldability and resistance to sour gas have been met in commercial productions through optimization of steel chemistry and intensified reduction of phosphorus, sulfur and inclusions^{1,2}. Since the optimum use of calcium or rare earths for metal treatment were adopted, the resistance to Hydrogen Embrittlement (HE), Hydrogen Induced Cracking (HIC) and Sulfide Stress Cracking (SSC) have been markedly improved³. To achieve the satisfactory performance in a line-pipe steel in service, it is necessary to ensure first that the steel possesses sufficient strength to sustain the design stress without yielding; secondly, that it possesses sufficient fracture toughness to resist fast fracture; thirdly, that it does not suffer disastrous impairment of its fracture resistance (in this case, resistance to HE, HIC and SSC) by the action of the chemical environment in which it operates (in this case, the sour hydrocarbons). Considerable works on the problems of HIC and SSC of line-pipe steels have been

conducted to date³⁻⁶. However, little work has been done with respect to the effect of the dissolved hydrogen on the fracture toughness of these new steels. The present work is concerned with the effect of both non-metallic inclusions and dissolved hydrogen on the fracture toughness and fracture mechanism in four different line-pipe steels used for the transport of natural sour hydrocarbons.

II. EXPERIMENTAL PROCEDURES

The materials for the study were obtained from four low-strength carbon-manganese API-5L Grade X52 (two treated with calcium) steel pipes. These pipes were selected as representative of steels used in existing natural hydrocarbons transmission pipelines. The pipe diameter was 91.40 cm (36 in) and the wall thickness was 2.07 cm (0.81in); all specimens were prepared without flattening. The chemical composition of the pipes is presented in Table 1; the pipes A and C are treated with calcium and belong to the new type of API of steels for sour hydrocarbons, whereas pipes B and D are traditional API X52 steels with low and high sulfur respectively. Metallographic specimens were examined using optical and scanning electron microscopy.

Table 1. Chemical Composition of the Pipes in Weight Percent

Pipe	C	Si	Mn	P	S	Ca
A	0.08	0.22	1.02	0.04	0.008	0.004
B	0.12	0.21	1.05	0.03	0.008	---
C	0.03	0.26	1.08	0.04	0.002	0.003
D	0.21	0.60	1.20	0.03	0.036	---

The fracture toughness was determined for axial and circumferential crack growth at room temperature following ASTM E813-87 recommended procedure for J_{IC} testing. The compact tension specimen geometry with side grooves was employed, with thickness $B = 17$ mm, net thickness $B_n = 14$ mm and width $W = 50.8$ mm. The specimens were fatigue pre-cracked to a crack length of $a/W \approx 0.55$, with a R ratio of 0.1 and an initial ΔK value of $14 \text{ MPa m}^{-1/2}$, subsequently adjusted to maintain an approximated fatigue crack growth rate of $3 \times 10^{-5} \text{ mm/cycle}$. An effective elastic modulus $E/(1-\nu^2)$, where E is Young's modulus and ν is Poisson's ratio, of 180,000 MPa allowed satisfactory monitoring of the crack length from the elastic compliance. This same value was also employed to calculate K_{IC} values from the measured J_{IC} values.

Hydrogen charging was carried out following NACE Standard TM0177-90 using NACE solution B. The pH of the H_2S saturated solution was 3.02. Prior to hydrogen charging the CT samples were polished to 1200 grade silicon carbide paper and were degreased in acetone. The NACE test solution was purged with argon for 1 h to reduce the dissolved oxygen content. Immediately after purging, a H_2S flow of 200 ml/min per liter of solution was bubbled through the solution for 1 h to ensure that the solution was fully saturated, then, the H_2S flow was decreased to 10 ml/min per liter of solution to maintain the saturation. The total

charging time at room temperature was 12, 24, 48 and 72 h. When charging was completed, a thin layer of copper from a saturated CuSO₄ solution was plated onto the specimens to prevent hydrogen escape.

III. RESULTS AND DISCUSSION.

Microstructure

The inclusion morphology in the longitudinal direction (rolling direction) is shown in Figure 1. Inclusions in pipes A and C showed a spherical morphology; whereas the pipes B and D contained elongated inclusions. Qualitative EDS microanalysis indicated that the spherical inclusions observed in pipes A and C, have a center rich in MnS surrounded by a continuous rim rich in CaS (Figure 2). The elongated inclusions observed in pipes B and D are formed by MnS. The microstructure in the three pipe directions are shown in Figure 3. The microstructures were ferrite and pearlite in banded structures along the rolling direction.

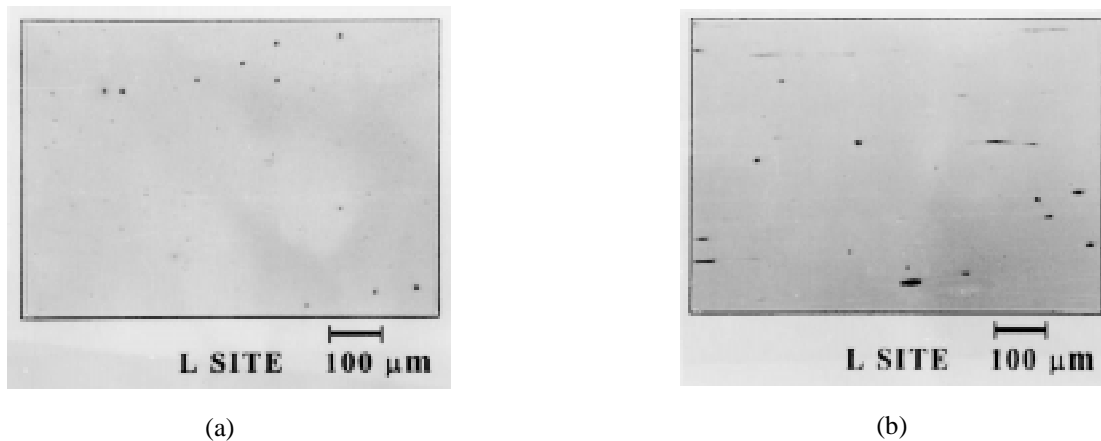


Figure 1. a) spherical inclusions observed in pipes A and C, b) elongated inclusions observed in pipes B and D.

A quantitative metallographic evaluation using light microscopy, scanning electron microscopy, and an Pro-Image II image analyzer was undertaken to quantify metallographic parameters characterizing inclusions and phases for the four pipes. The parameters measured were the size and volume fraction of inclusions (V_f), the center to center inclusion spacing (λ), ferrite and pearlite volume fraction (V_f) and the grain size. These results are summarized in Table 2.

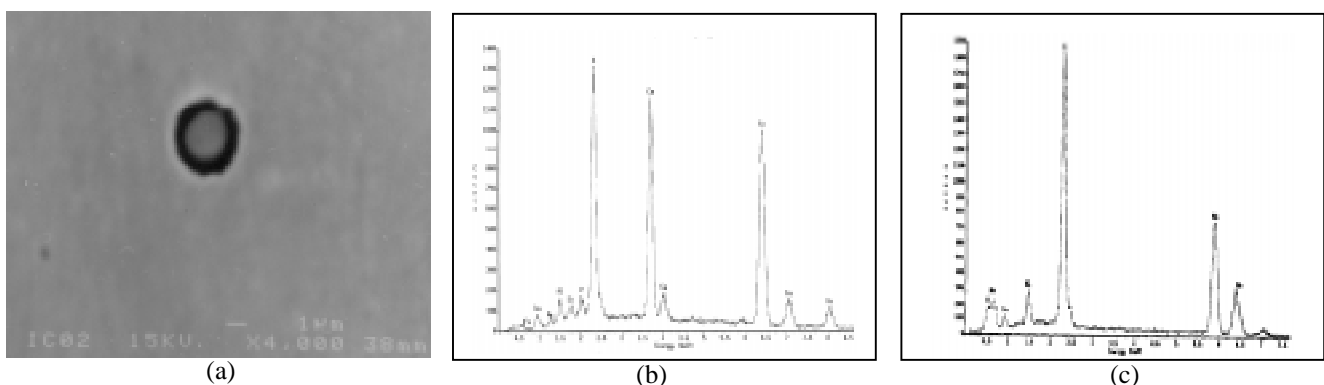


Figure 2. a) SEM micrograph of the spherical inclusions observed in pipes A and C, b) EDS spectra of the inclusion dark rim, c) EDS spectra of the inclusion gray center.

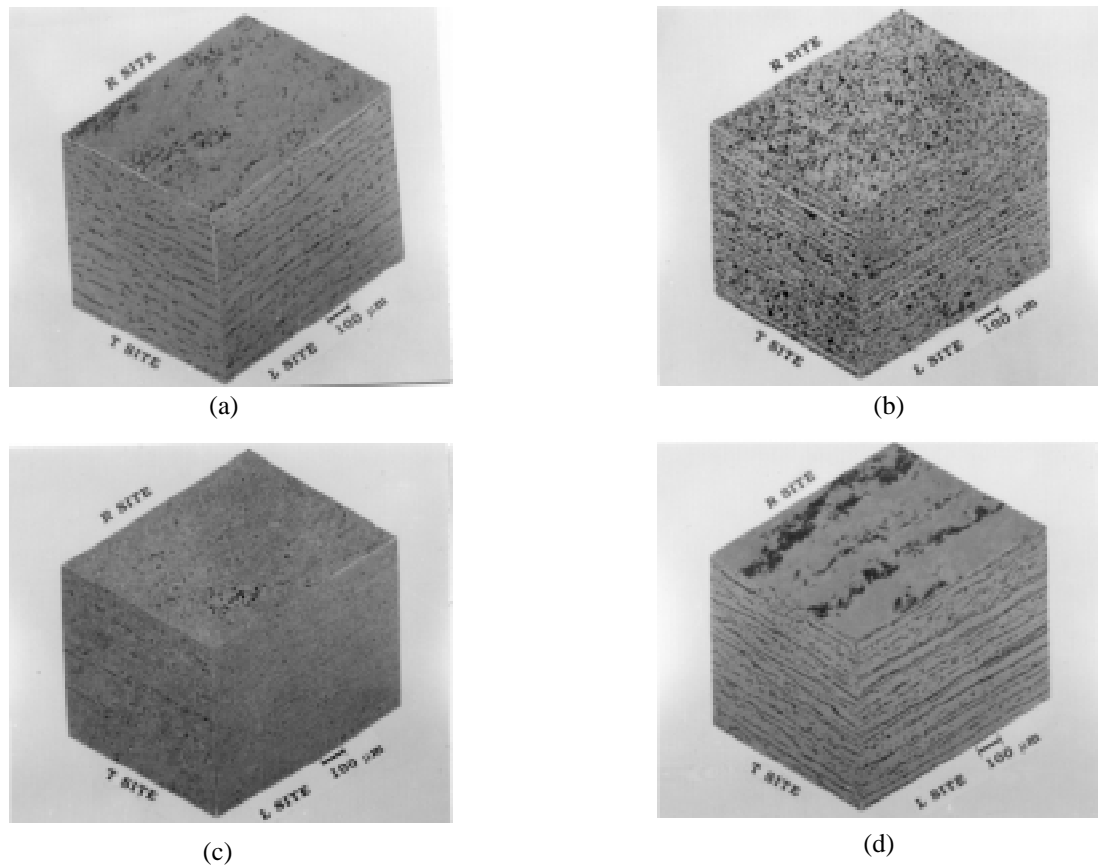


Figure 3. Three dimensional micrographs showing the microstructure and orientation of the pipe-line steels, a) pipe A, b) pipe B, c) pipe C, d) pipe D.

Table 2. Microstructural Parameters Determined by Quantitative Metallographic Analysis

Pipe	Inclusions Morphology	Inclusions Size (μm)	Inclusions V_f	λ (μm)	Ferrite V_f	Pearlite V_f	ASTM Grain Size
A	Spherical	4	0.0005	100	80	20	7
B	Elongated	5	0.0005	110	80	20	6
C	Spherical	2	0.0001	300	90	10	9
D	Elongated	10	0.001	80	75	25	7

The spherical shape of the inclusions in the steels A and C is attributed to the effect of calcium on MnS inclusion morphology[]; and because of this, it is expected that steels A and C will be less susceptible to hydrogen embrittlement than steels B and D. Table 2 shows that the metallographic parameters of steels A and B are quite similar, the only difference being the inclusion morphology, which agrees with the chemical composition of both steels. Pipe D showed the highest sulfur content and the highest volume fraction and size of elongated inclusions; whereas, the low sulfur steel (pipe C) showed a very low volume fraction of fine spherical inclusions.

Fracture Toughness

The fracture toughness values are reported in Table 3. The four steels showed anisotropy in the fracture toughness, being greater in the radial direction. As expected, the steels treated with calcium (steels A and C)

exhibited higher levels of fracture toughness than the conventionally processed steels (steels B and D), being the low sulfur steel the one that exhibited the highest fracture toughness in both directions. The fracture toughness of hydrogen-charged samples was lower than the values for the uncharged samples in both test directions.

Table 3. Fracture Toughness Values

PIPE	Hydrogen charging time(h)	J_{IC} (KJ/m^2)		K_{JC} ($MPa m^{1/2}$)	
		Axial crack propagation	Circumferential Crack propagation	Axial crack propagation	Circumferential Crack propagation
A	0	540.5*	832*	353.5*	438.5*
	12	187.5	301	208.1	263.8
	24	190	345	209.5	282.2
	48	177	314	202.3	269.3
B	0	400*	636*	304.1*	383.5*
	12	121.5	206	167.4	216.3
	24	62.5	215	120.1	256.6
	48	63.5	210	121.1	220.3
C	0	724*	1000*	409*	480.9*
	12	679*	825*	395*	436.7*
	24	673*	823*	397.4*	436.6*
	48	635*	805.5*	387.7*	431.5*
D	0	66	240.5	123.5	235.4
	12	31.5	32.5	85.3	86.6
	24	29.5	36.5	82.6	91.9
	48	29.5	37	82.1	92.4

*Close to valid values

Figures 4a and 4b show the variation of the fracture toughness, K_{JC} , as a function of the hydrogen charging time, for the pipe-line steels in the longitudinal and circumferential directions respectively. As shown by Figures 4a and 4b, the K_{JC} values of the hydrogen-charged materials, sharply drop in the first 12 h of charging, with respect to those of the hydrogen-uncharged materials, principally in the case of the steels A, B and D. After 12 h. of hydrogen charging, the K_{JC} values were almost constant. This indicates that these steels reached the hydrogen saturation after 12 h of charging. In the case of steel C, which was treated with calcium and had a low sulfur content, the K_{JC} values of the hydrogen-charged samples decreased slightly with respect to those of the hydrogen-uncharged samples.

Some authors have reported that elongated MnS inclusions are strong hydrogen traps, which produces a high hydrogen embrittlement susceptibility in pipe-line steels^{1,2}. Fracture toughness results showed that steel B is more susceptible to hydrogen embrittlement than steel A, whereas metallographic characterization showed that the metallographic parameters of steels A and B are quite similar; the only difference being the inclusion morphology, which was spherical in the case of steel A and elongated in the case of steel B. These results suggest that controlling the shape of the sulfide inclusions to the spherical type by addition of calcium decrease the detrimental effect of hydrogen on fracture toughness of pipe-line steels.

Comparing the K_{JC} values of the two steels treated with calcium, we can see that the steel A is markedly more susceptible to the hydrogen embrittlement than steel C. Both steels have spherical inclusions and the main difference between them is that steel A has a higher inclusions volume fraction than steel C. Therefore, these results suggest that controlling the shape of the sulfide inclusions to the spherical type by addition of calcium is not enough to minimize the detrimental effect of hydrogen on fracture toughness of pipeline steels, but at the same time the volume fraction of non-metallic inclusions has to be controlled, even if they have a spherical shape.

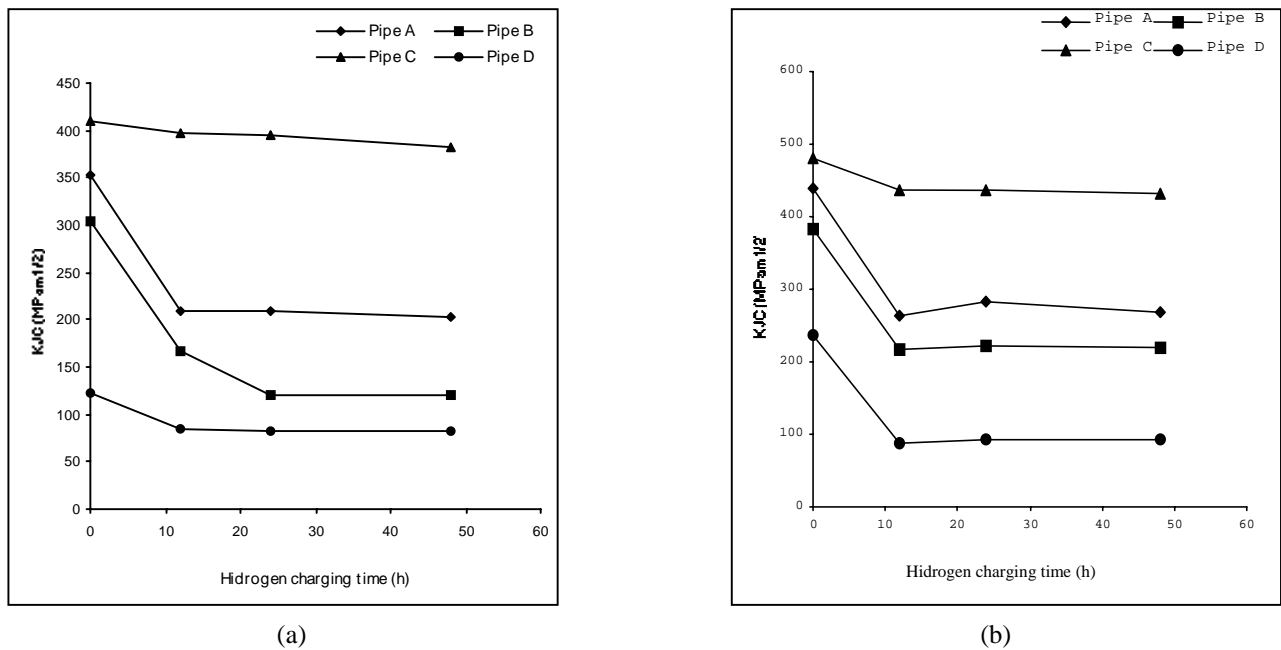
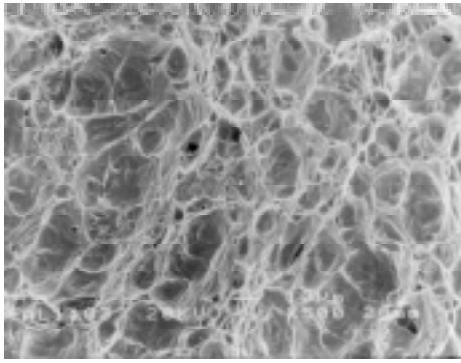
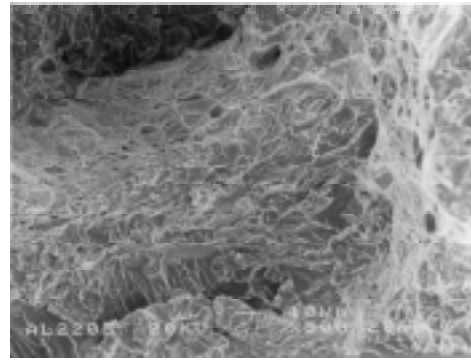


Figure 4. Effect of the hydrogen charging time on the fracture toughness values, K_{JC} , of the pipe-line steels; a) axial crack propagation; b) circumferential crack propagation.

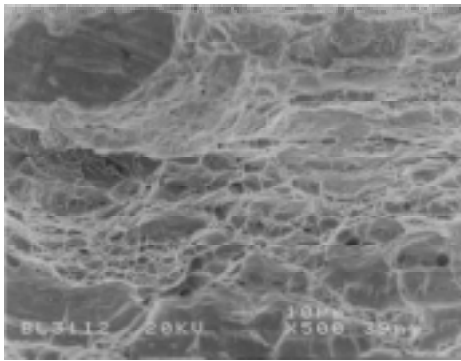
The fracture surfaces of the fracture toughness specimens were studied by scanning electron microscopy. Macroscopically, the fracture surfaces of uncharged samples had a rough fibrous appearance. Microscopically, they presented a ductile fracture consisting of dimples produced by microvoid coalescence and there was no trace of cleavage fracture. The dimples were originated at the non-metallic inclusions. Axial samples of steels B and D showed elongated dimples; whereas circumferential samples showed equiaxial dimples. The fracture surfaces of steels A and C were formed by equiaxial dimples in both longitudinal and circumferential test directions. The reduction of fracture toughness by hydrogen was accompanied by a change in fracture mode. Figure 5 compares the fracture surface of the J_{IC} specimens. In this figure it is seen that the fracture of the hydrogen charged samples was far less ductile and exhibited a mixture of ductile fracture and large cleavage or quasi-cleavage areas. For the steel C, the surface fraction of cleavage was substantially smaller than that observed in steels A, B and D, while for the traditional API X-52 steel (steel D with relatively high sulfur content and elongated MnS inclusions), the surface fraction of cleavage was quite high.



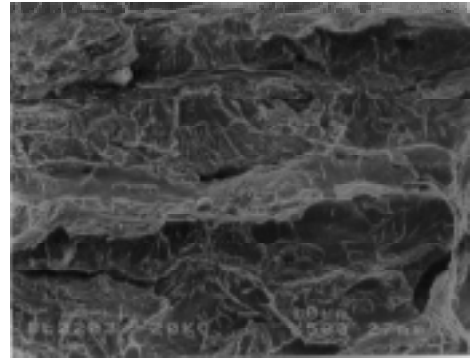
(a)



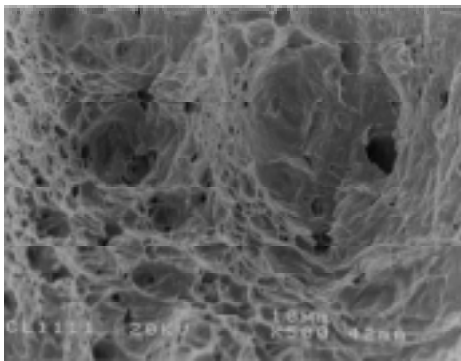
(b)



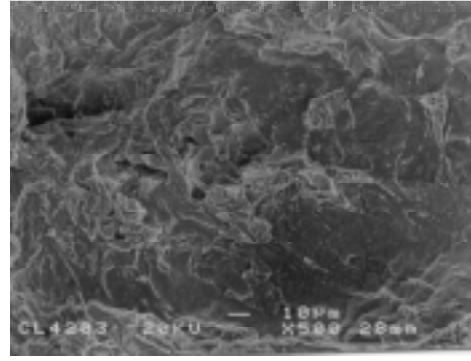
(c)



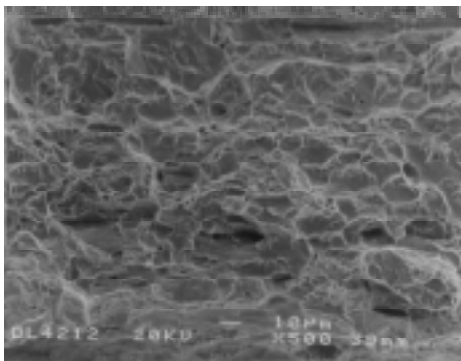
(d)



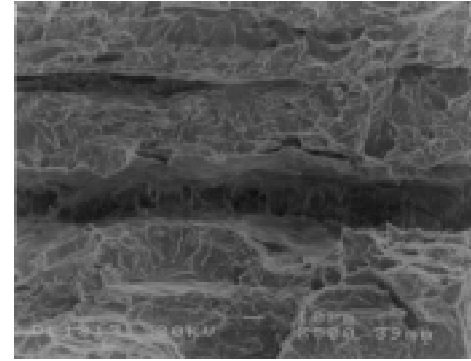
(e)



(f)



(g)



(h)

Figure 5. Examples of the fracture surfaces of the J_{IC} specimens with the crack propagation in the axial direction; a) pipe A uncharged (UC), b) pipe A hydrogen-charged (HC), c) pipe B UC, d) pipe B HC, e) pipe C UC, f) pipe C HC, g) pipe D UC, h) pipe D HC.

Table 4. Surface Fraction of Cleavage Observed on the Fracture Surface of Hydrogen-Charged Samples

Pipe A	Pipe B	Pipe C	Pipe D
0.35-0.40	0.52-0.60	0.21-0.25	0.89-0.95

IV. CONCLUSIONS

1. Controlling the shape of the MnS inclusions to the spherical type by addition of calcium decrease the detrimental effect of hydrogen on fracture toughness of pipe-line steels
2. Controlling the shape of the sulfide inclusions to the spherical type is no enough to minimize the detrimental effect of hydrogen on fracture toughness of pipeline steels, but at the same time the volume fraction of non-metallic inclusions has to be controlled, even if they have a spherical shape
3. The reduction of the API X-52 pipe-line steels fracture toughness by hydrogen dissolved is accompanied by a change in fracture mode, from ductile to a mixture of ductile and cleavage or quasi-cleavage.

REFERENCES

- 1) G. Herbsleb, R. K. Poepperling, and W. Schwenk, "Occurrence and Prevention of Hydrogen Induced Stepwise Cracking and Stress Corrosion Cracking of Low Alloy Pipeline Steels", Corrosion, NACE, 1981, Vol. 36, No. 5, pp. 247-256.
- 2) J. Charles, V. Lemoine, G.M. Pressouyre, "Metallurgical Parameters Governing HIC and SSC Resistance of Low Alloy Steels", Corrosion Convention, Houston, Texas, 1986, March 17-21, paper 164, pp.1-14
- 3) T. Taira, K. Tsukada, Y. Kobayashi, H. Inagaki and T. Watanabe "Sulfide Corrosion Cracking of Linepipe for Sour Gas Service", Corrosion-NACE, 1981, Vol. 37, pp.5-16
- 4) H.Y. Liou, R. I. Shieh, F.I. Wei, and S. C. Wang, "Roles of Microalloying Elements in Hydrogen Induced Cracking Resistant Property of HSLA Steels", Corrosion, 1993, Vol. 49, pp. 389-398
- 5) M. Kimura, N Totsuka, T. K. Amano, J. Matsuyama and Y. Nakai, "Sulfide Stress Corrosion Cracking of Line Pipe", Corrosion, 1989, Vol. 45, pp. 340-346.
- 6) R. W. Revie, V.S. Sastri, G.R. Hoey, R.R. Ramsingh, D.K. Mak and T. Shehata, "Hydrogen – Induced Cracking of Linepipe Steels Part 1-Threshold Hydrogen Concentration and PH", Corrosion, 1993, Vol. 49, pp 17-23.

ACKNOWLEDGEMENTS

Authors thank to the Instituto Politécnico Nacional, Pemex Exploración Región Sur for their support for the development of this work. This work was financed by PEP Region Sur, grant SRS GCTO 002/98.